Journal of the European Ceramic Society 22 (2002) 2437–2442
www.elsevier.com/locate/jeurceramsoc

Cooperative grain-boundary sliding in polycrystalline ceramics

H. Muto*, Y. Takahashi, T. Futami, M. Sakai

Department of Materials Science, Toyohashi University of Technology, Tempaku-cho, Toyohashi 441-8580, Japan

Received 7 October 2001; received in revised form 10 December 2001; accepted 20 February 2002

Abstract

The microscopic processes and mechanisms are investigated for the superplastic deformation of 3mol% yttria-partially stabilized tetragonal zirconia polycrystals. Tensile tests are carried out by the use of test specimens with various dimensions in order to examine the "specimen size effect" on stress–strain curve. The formation and development of surface corrugation on tensile specimens induced during superplastic deformation are carefully studied as a function of tensile strain. New findings, i.e. the "specimen size effect" and the "surface corrugation" are discussed in terms of the concept of cooperative grain-boundary sliding as a candidate for superplastic deformation and flow of polycrystalline materials.

Keywords: Mechanical properties; Superplastic deformation

1. Introduction

The science and engineering of superplastic deformation has been steadily growing and yielding attractive fields including the continuum- and micro-mechanics, practical applications to superplastically molding engineering components, etc. since the discoveries of huge elongation in an metallic alloy[1] and also in a ceramic material[2] were reported. Although plenty of models for grain-boundary sliding during superplastic deformation have been proposed,[3–11] these are not sufficient enough to understand the most important feature of superplastic deformation, i.e. no necking during a large-scale elongation.

The most plausible candidate of microscopic processes for the superplastic deformation of polycrystalline materials may be cooperative grain-boundary sliding (CGBS), occurring through the cooperative movement of grain groups.[6–15] A series of studies for CGBS have been conducted by many scientists, since the work of Ball and Hutchison in 1969.[6] Theoretical considerations and experimental works for CGBS mechanisms have also been made by the present authors.[12–16] They concluded from the view point of the principle of minimum energy dissipation that the cooperative sliding of grain groups along grain-boundaries is essential to the large-scale superplastic deformation of polycrystalline materials.[12]

The intent of this paper is to examine in experiment the microscopic processes and mechanisms in the superplastic deformation of a 3 mol% yttria-partially stabilized tetragonal zirconia polycrystal (3Y-TZP). Mainly scrutinized are the theoretical prediction of "test specimen size effect"[13] as well as the microscopic processes for the formation and development of surface corrugation that is induced during superplastic elongation.[15]

2. Experimental

2.1. Materials

The 3Y-TZP used in this work was supplied from Nikkato Co. Ltd., Japan. It has a mean grain diameter of 0.3 μm, being small enough to exhibit well-defined superplastic deformation. Soda-lime glass (SL-glass) was also used as a reference material, for it has none of grain structures and exhibits a "linear" viscoelastic deformation and flow. Some characteristic properties of these materials are listed in Table 1.

2.2. Tensile test

3Y-TZP and SL-glass plates were machined to tensile specimens with the dimensions depicted in Fig. 1; the

* Corresponding author. Tel.: +81-532-44-6800; fax: +81-48-5833.
E-mail address: muto@tutms.tut.ac.jp (H. Muto).

0955-2219/02/$ - see front matter
PII: S0955-2219(02)00102-4

gage length λ_0 of 30 mm and the cross-sectional area A_0 ($=B_0 \times W_0$) ranging from 3 mm^2 (1×3 mm) to 36 mm^2 (6×6 mm). The detailed dimensions of test specimens labeled as A, B, C, D and E are listed in Table 2.

Tensile tests were conducted by a conventional Instron-type testing machine (Sanwa Kiki Co. Ltd., Toyohashi, Japan) equipped with an electric furnace with SiC heating elements. The load P and the strain ϵ during tensile testing were measured by a water-cooled load cell (TCLZ-200KA, Tokyo Sokki Co. Ltd., Tokyo, Japan) and a laser-speckle extensometer, respectively. Detailed setup of the test system was reported in the literature.[15,16] The tensile tests were conducted under a constant crosshead speed of 0.05 mm/min at 570 °C for SL-glass and of 0.02 mm/min at 1300 °C for 3Y-TZP.

A consecutively repeated tensile test was also conducted for 3Y-TZP under a constant crosshead speed of 0.03 mm/min at 1300 °C. The first run in this repeated test was terminated at the tensile strain of 0.2, and then, the specimen was removed out of the furnace. The profile of the corrugation induced on the side surface of elongated specimen was measured by a surface roughness meter (SURFTEST SV-600, Mitsutoyo Co. Ltd., Kawasaki, Japan). After the measurement of surface corrugation, this specimen was set again in the furnace to conduct the second repeated tensile test to the strain ε of 0.5, and then, the third run to $\varepsilon = 0.75$. The measurement of the profile of surface corrugation thus conducted in the respective test runs elucidates how the surface corrugation forms and develops during elongation. Their stress vs. strain curves (S–S curves) were also measured in these repeated tests.

Table 1
Some properties of the ceramics used in this work

	Young's modulus (GPa)	Mean grain size	Density (g/cm^3)
SL-Glass	74	–	2.51
3Y-TZP	210	0.3	6.04

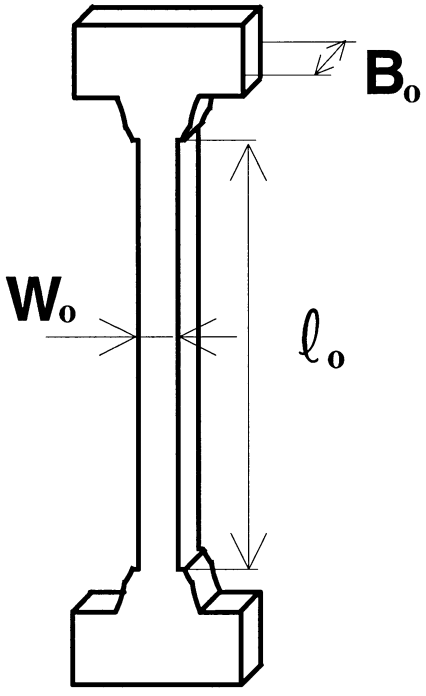

Fig. 1. Geometry of test specimen.

2.3. Microstructural observation

The microstructural observations were made by scanning electron microscopy (SEM) after tensile testing. A part of the gauge section cut out of a deformed tensile specimen was surface-finished with diamond paste (1 μm grains). After thermally etching the polished surface, the microstructural changes induced during elongation were carefully examined on the etched surface.

3. Results

3.1. S–S curve

The relationships of the S–S curves obtained for test specimens with various dimensions are plotted for SL-

Table 2
Dimension of tensile specimen

	ℓ_0 (mm)	B_0 (mm)	W_0 (mm)	A_0 ($=B_0 \times W_0$) (mm)
A	30	1	3	3
B	30	2	2	4
C	30	3	3	9
D	30	4	4	16
E	30	6	6	36

SL-Glass: A,B,C,D; 3Y-TZP: A,B,C,D,E.

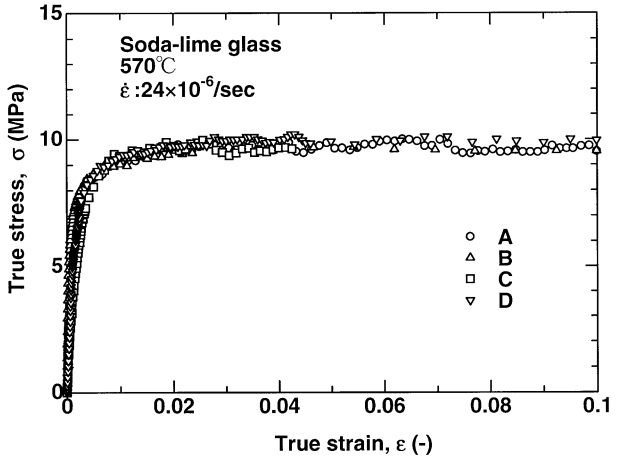

Fig. 2. S–S curves of SL-glass for test specimens with various dimensions.

glass in Fig. 2 and for 3Y-TZP in Fig. 3, respectively. The strain rates $\dot{\varepsilon}$ are 24×10^{-6} s^{-1} and 8.5×10^{-6} s^{-1} for SL-glass and 3Y-TZP, respectively. It is a very natural consequence in linear viscoelastic materials that gives none of test specimen size effect on the S–S curve, as actually seen in Fig. 2 for SL-glass. However, the S–S curves of 3Y-TZP do depend on the size of test specimen (see Fig. 3). Specimen with a larger cross-sectional area A_0 is more easily deformable than that with a smaller one. A similar size-effect was reported by Astanin et al.[17] The microstructural inspection in the elongated specimens confirmed no changes in the size and shape of individual grains, implying the insignificance of the conventional accommodation processes and mechanisms of lattice/grain-boundary diffusion and solution–redeposition.

3.2. Surface profile

As reported in the literature, surface corrugation is well-developed even at a small strain of 0.2 in 3Y-TZP.[15] The profiles of surface corrugation induced at the tensile strains of 0.2, 0.5 and 0.75 are shown in Fig. 4, as the relations between surface depth h and relative location x. It must be noticed in Fig. 4 that (1) the surface corrugation is enhanced with the increase in strain (elongation), and (2) individual ridge of surface elongation is distorted and split into double or triple ridges when the applied strains exceed 0.5. We must emphasize here that no surface corrugation was obviously observed in SL-glass. Accordingly, this surface corrugation is an essential phenomenon associated with the superplastic deformation of polycrystalline materials.

The S–S relations in the repeated tests are given in Fig. 5, showing that the resistance to deformation increases with the repetition (i.e., with the increase in the "total" strain).

4. Discussion

Most of models and theories as to the microscopic processes and mechanisms for superplastic deformation and flow can not realize the present test results; (1) the deformation resistance to tensile elongation significantly depends on the initial cross-sectional area A_0 of test specimen (see Figs. 3 and 5), and (2) a periodic surface corrugation is induced and developed on the surface of test specimen during elongation (see Fig. 4). As addressed in the preceding section, no morphological changes in the grains were observed even at large elongation. The present test results, therefore, suggest that a major part of the macroscopic strain may be accommodated by CGBS processes.[6–15]

Quantitative examinations on CGBS have been conducted by the present authors.[12–15] Schematic illustration of this CGBS under tensile loading is depicted in

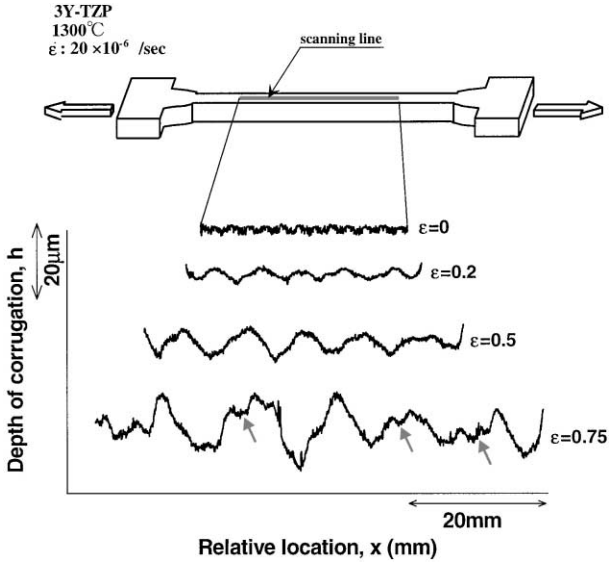

Fig. 4. Surface profiles at various tensile strains ranging from 0.2 to 0.75 obtained in a repeated tensile test.

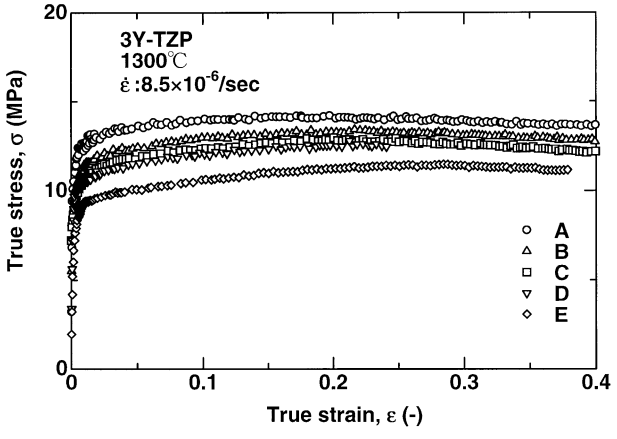

Fig. 3. S–S curves of 3Y-TZP for test specimens with various dimensions.

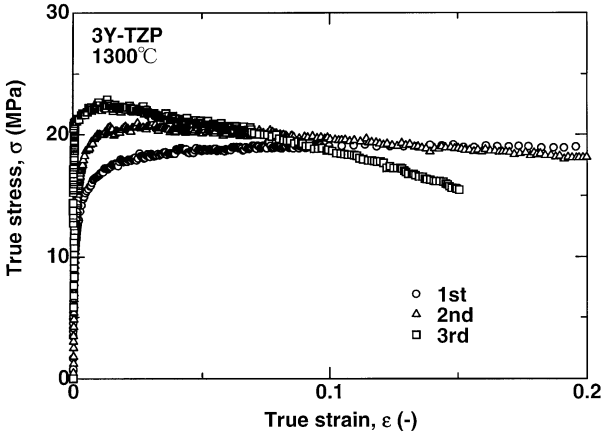

Fig. 5. S–S curves in the sequentially repeated tensile test.

Fig. 6. When a two-dimensional close-packed aggregate [Fig. 6(a)] was subjected to a tensile stress, the groups of grains shaping regular triangles start counter sliding each other [Fig. 6(b)] along the boundaries of each triangle. The first stage of CGBS brings the process to completion at the close-packed configuration of the second stage [Fig. 6(c)]. This CGBS goes on during large-scale elongation with a sequential reduction in the size of cooperative triangles until the grains are rearranged in to a single linear array.[12,13] The deformation energy $\Delta U(\varepsilon)$ which is required to overcame grain interlocking on sliding planes is expressed by[13]

$$\Delta U(\varepsilon) = \frac{8}{3}\left(2-\sqrt{3}\right)^2 K\left[\frac{R}{L(\varepsilon)}\right]^2 \quad (1)$$

where, R and $L(\varepsilon)$ are the radius of grain and the sliding length at a tensile strain of ε, respectively. The parameter K is the bulk modulus of individual grains. Eq. (1) means that the resistance to superplastic deformation through overcoming interlocking stresses is proportional to R^2 and to $[L(\varepsilon)]^{-2}$. In other word, the stress for superplastic deformation will be increased with the increase in grain size R, and with the decrease in the length of grain-boundary sliding $L(\varepsilon)$. It must be noticed that the length $L(\varepsilon)$ is proportional to the global dimension D_0 of the original test specimen due to the geometrical similarity between D_0 and $L(\varepsilon)$. Accordingly, we have the proportionalities of $\Delta\ U(\varepsilon) \propto [L(\varepsilon)]^{-2}$ D_0^{-2} implying the presence of the test specimen size-effect on superplastic deformation, i.e. the resistance to superplastic deformation will increase with the decrease in the size of test specimen.

The results of S–S curves of 3Y-TZP with various dimensions shown in Fig. 3 are sufficient enough to support this theoretical prediction. The global dimensions B_0 and W_0 for specimen E are the largest of all the test specimens. Therefore, the resistance energy $\Delta U(\varepsilon)$ to overcame grain interlocking will be the smallest due to the proportional relationship of $\Delta U(\varepsilon)$ D_0^{-2}, making the deformation and flow easiest. A similar dimensional argument is also applicable to the result in the repeated tensile test; the dimensions of B_0 and D_0 in the first run of tensile test are the largest of all the repeated tensile tests, resulting in the smallest resistance to deformation (see Fig. 5).

Most of the conventional accommodation processes and mechanisms reported in the literature[1,3–5,18–21] always allow a homogeneous deformation (an affine deformation) where each microscopic element in a macroscopic body has the same strain tensor and the rotation tensor as every other element. This fact leads to a very uniform and smooth surface profile during the elongation of the body, such as the smooth surfaces of SL-glass in viscoelastic deformation and flow. Accordingly, the corrugation that is induced on the surface of 3Y-TZP (Fig. 4) is neither understood nor expected in the conventional frameworks of superplasticity. Similar surface profiles of corrugation were also reported for metals,[22] and a nanocrystalline 3Y-TZP.[23] The corru-

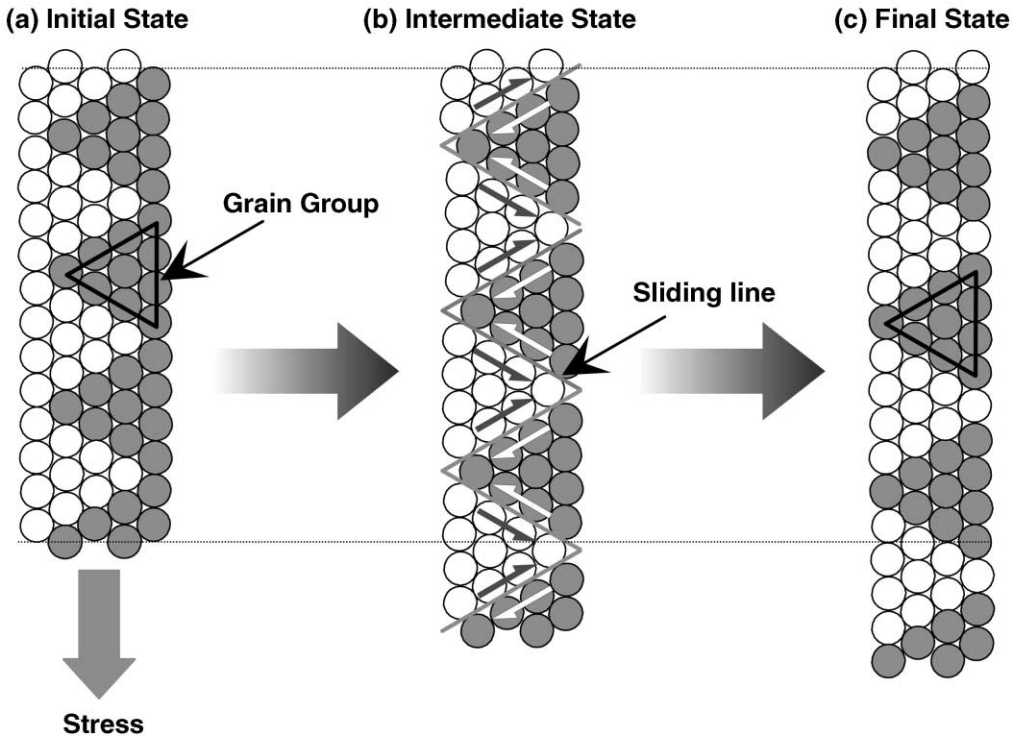

Fig. 6. Schematic illustration of the concept for CGBS under tensile loading.

gation induced on the surface signifies that very localized inhomogeneity in microscopic as well as macroscopic senses is essential to superplastic deformation and flow.

As a matter of fact, the localized inhomogeneity associated with large-scale deformation is the essence of the present model of CGBS as demonstrated and emphasized in Fig. 6 as well as discussed in the literature.[12–15] One of possible processes and mechanisms which may result in a periodical surface corrugation is schematically illustrated in Fig. 7 on the basis of the present CGBS model. Periodical formation of slip bands along the boundaries of cooperative grain groups may result in the surface corrugation.

Upon the corrugation being well developed under the strain of $\varepsilon = 0.5$ shown in Fig. 4, the troughs of corrugation became locally hardened, and the ridges are locally softened. This is caused from the dimensional difference between the mean sliding lengths $L(\varepsilon)$ of troughs and of ridges; $L(\varepsilon)$ at troughs is always smaller than that at ridges. Accordingly, the ridges are more susceptible to deformation, and vice versa at the location of troughs. This fact will make the deformation at ridges more active, and then result in splitting each ridge into double or triple ridges, as shown by the arrows in Fig. 4 for $\varepsilon = 0.75$. These local hardening and softening processes via the CGBS-induced local inhomogeneity would be the supression of necking during superplastic deformation, which is one of the most essential features of this type of large-scale deformation.

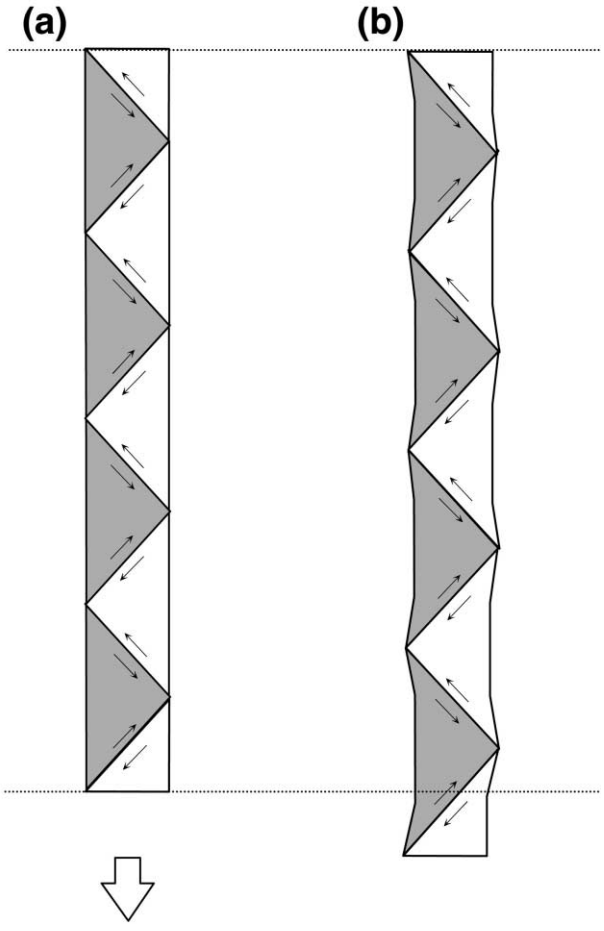

Fig. 7. Schematic illustration of the model for surface corrugation associated with the CGBS process.

Further studies must be made in near future for deeper understanding the CGBS in superplastic deformation: (1) the geometrical factors to dictate the periodicity of surface corrugation, (2) profiles of surface corrugation in terms of large-scale strains exceeding $\varepsilon = 1.0$, and (3) the effect of microstructures (size and shape of grains, liquid phase at grain-boundaries, etc.) on the profile of corrugation.

5. Conclusion

The deformation processes and mechanisms for large-scale deformation have been experimentally examined by the use of 3Y-TZP in tensile tests. New findings include; the deformation resistance to tensile elongation significantly depends on the initial cross-sectional area of test specimen, and a periodic surface corrugation is induced and developed on the surface of test specimens during elongation. These results were well-characterized in terms of the concept of CGBS model. It was concluded that the CGBS is the most plausible candidate for microscopic accommodation processes in the superplastic deformation of polycrystalline materials.

Acknowledgements

A part of this work was supported by Japan Society for the Promotion of Science (The Grant-in-Aid for Scientific Research (A), # 12305043), and also by The Nippon Sheet Glass foundation for Materials Science and Engineering.

References

1. Pearson, C. E., Viscous properties of extruded eutectic alloys of Pb-Sn and Bi-Sn. *J. Inst. Metals*, 1963, **54**, 111–123.
2. Wakai, F., Sakaguchi, S. and Matsuno, Y., Superplasticity of yttria-stabilized tetragonal ZrO_2 polycrystals. *Adv. Ceram. Mater.*, 1980, **1**, 259–263.
3. Ashby, M. F. and Verrall, R. A., Diffusional-accommodated flow and superplasticity. *Acta Metall.*, 1973, **21**, 149–163.
4. Gifkins, R. C., Grain boundary sliding and its accommodation during creep and superplasticity. *Mater. Trans.*, 1976, **7A**, 1225–1232.
5. Gifkins, R. C., Grain rearrangement during superplastic deformation. *J. Mater. Sci.*, 1978, **13**, 1926–1936.
6. Ball, A. and Hutchison, M. M., Superplasticity in the aluminum-zinc eutectoid. *Metal Sci. J.*, 1969, **13**, 1–6.

7. Zelin, M. G. and Mukherjee, A. K., Cooperative phenomena at grain boundaries during superplastic flow. *Acta Metall. Mater.*, 1995, **43**(6), 2359–2372.
8. Zelin, M. G. and Mukherjee, A. K., Geometrical aspects of superplastic flow. *Mater. Sci. Eng.*, 1996, **A208**, 210–225.
9. Zelin, M. G. and Mukherjee, A. K., Study of cooperative grain boundary sliding by using macroscopic marker lines. *Metall. Mater. Trans.*, 1995, **26A**, 747–750.
10. Astanin, V. V., Sisanbaev, A. V., Pshenichnyuk, A. I. and Kaibyshev, O. A., Self-organization of cooperative grain boundary sliding in aluminum tricrystals. *Scripta Mater.*, 1997, **36**, 117–122.
11. Zelin, M. G., Krasilnikov, N. A., Valiev, R. Z., Grabski, M. W., Yang, H. S. and Mukherjee, A. K., On the microstructural aspects of the nonhomogenity of superplastic deformation at the level of grain groups. *Acta Metall. Mater.*, 1993, **42**, 119–126.
12. Sakai, M. and Muto, H., A novel deformation process in an aggregate: a candidate for superplastic deformation. *Scripta Mater.*, 1998, **38**, 909–915.
13. Muto, H. and Sakai, M., The large-scale deformation of polycrystalline aggregates: cooperative grain-boundary sliding. *Acta Mater.*, 2000, **48**, 4161–4167.
14. Muto, H. and Sakai, M., A novel deformation mechanism for superplastic deformation. *Key Eng. Mater.*, 1999, **166**, 103–108.
15. Muto, H. and Sakai, M., Deformation-induced surface corrugation of superplastic ceramics. *J. Mater. Res.*, 2001, **16**, 1879–1882.
16. Muto, H. and Sakai, M., Application of speckle strain mater to viscoelastic study of ceramic materials. *J. Ceram. Soc. Japan*, 2000, **108**, 673–676 (in Japanese).
17. Astanin, V. V., Padmanabhan, K. A. and Bhattacharya, S. S., Model for grain boundary sliding and its relevance to optimal structural superplasticity. Part 3—effect of flow localization and specimen thickness on superplasticity in alloy Supral 100. *Mater. Sci. Technol.*, 1996, **12**, 545–550.
18. Nabarro, F. R. N., Steady state diffusional creep. *Phil. Mag. A*, 1967, **16**, 231–237.
19. Coble, R. L., A model for boundary diffusion controlled creep in polycrystalline materials. *J. Appl. Phys.*, 1963, **34**, 1679–1682.
20. Weetman, J., Steady state creep of crystals. *J. Appl. Phys.*, 1957, **28**, 1185–1191.
21. Raj, R. and Chyung, C. K., Solution-precipitation creep in glass ceramics. *Acta Metall.*, 1980, **29**, 159–166.
22. Partridge, P. G., McDarmaid, D. S. and Bowen, A. W., A deformation model for anisotropic superplasticity in two phase alloys. *Acta Metall.*, 1985, **33**, 571–577.
23. Yan, D. S., Zheng, Y. S., Gao, L., Zhu, C. F., Wang, X. W., Bai, C. L., Xu, L. and Li, M. Q., Localized superplastic deformation of nanocrystalline 3Y-TZP ceramics under cyclic tensile fatigue at ambient temperature. *J. Mater. Sci.*, 1998, **33**, 2719–2723.